Few Cycle Dynamics of Multiphoton Double Ionization

V. R. Bhardwaj, S. A. Aseyev, M. Mehendale, G. L. Yudin, D. M. Villeneuve, D. M. Rayner, M. Yu. Ivanov, and P. B. Corkum

National Research Council of Canada, Ottawa, Ontario, Canada K1A 0R6

(Received 2 August 2000)

In intense field ionization, an electron removed from the atomic core oscillates in the combined fields of the laser and the parent ion. This oscillation forces repeated revivals of its spatial correlation with the bound electrons. The total probability of double ionization depends on the number of returns and therefore on the number of optical periods in the laser pulse. We observed the yield of Ne^{2+} relative to Ne^{+} with 12 fs pulses to be clearly less compared to 50 fs pulses in qualitative agreement with our theoretical model.

DOI: 10.1103/PhysRevLett.86.3522 PACS numbers: 32.80.Rm

In strong field multiphoton ionization an electron, promoted to the continuum, oscillates in the laser field. This oscillation can result in repeated revivals of the spatial correlation between the bound electrons and continuum electron. In contrast, in single photon ionization no such revivals exist. This difference can influence double ionization. Two mechanisms dominate weak field single photon double ionization [1,2]. (i) *Shakeoff:* An electron is removed from the atom so rapidly that the remaining electron cannot adiabatically adjust to the new ionic potential resulting in some probability of ejection of the second electron; (ii) *interception:* An electron interacts with the second electron in a binary collision, on its way out, knocking both electrons free.

Direct parallels to these mechanisms have been suggested to explain multiphoton double ionization [3,4]. In addition, two uniquely strong field processes become possible. (1) *Collective tunneling* [5]: Both electrons tunnel together through the Coulomb barrier that is reduced by the laser field. (2) *Rescattering* [6]: An electron freed by tunneling is driven back to the parent ion during the next few optical cycles. In the collision that can occur a second electron is excited or knocked free, with excitation converted into ionization by the laser field. Ellipticity dependence measurements [7] along with recent measurements of recoil-ion momentum distributions of doubly charged He [8] and Ne [9] ions are in good accord with the rescattering model.

Within the recollision model, strong field double ionization should depend on the pulse duration for few cycle laser pulses. The dependence arises because of the long range Coulomb potential between the electron and parent ion. This potential causes a small deflection of large impact parameter electrons whenever they approach the ionic core and increases the probability for the electron to make a low impact parameter inelastic collision with the ionic core after multiple passes [10]—the so-called Coulomb focusing. In addition, the laser induced decay of the bound states excited by the recollision also contributes. We measured the yield of Ne^{2+} relative to Ne^{+} with 12 fs pulses to be ~60% of that of the yield for 50 fs. We expect larger differences for shorter pulses.

The motivation for the experiment is our calculations of double ionization of He (Fig. 1) which agree with the benchmark experimental data of [11] and make clear predictions on the sensitivity of double ionization to pulse duration due to Coulomb focusing.

Our model of double ionization is based on the rescattering mechanism [6,10] and is described in detail in [12]. Briefly, an electron tunnels out at any phase $\phi = \omega_L t$ of the laser field with probability weighted according to the standard tunneling formula [13], $W \propto \exp[-2(2I_p)^{3/2}/3E|\cos\phi(t)|]$. Here I_p is the ionization potential of the atom and E is the electric field amplitude. Motion of the electron after tunneling in the combined Coulomb and laser fields is calculated classically for

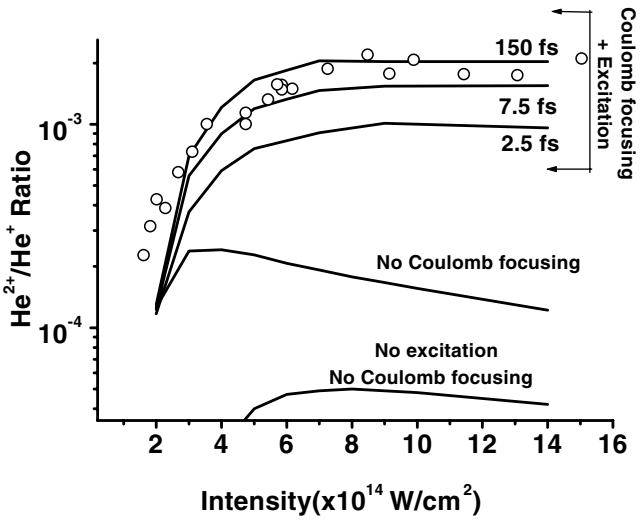

FIG. 1. Calculated ratio of doubly to singly charged He as a function of laser intensity. For the bottom curve neither Coulomb focusing nor collisional excitation were included. The next curve from the bottom includes all excitation channels. Top curves include both the Coulomb focusing and collisional excitation and demonstrate the role of late returns, implying pulse dependence. Circles are experimental data of [11].

 0031-9007/01/86(16)/3522(4)$15.00

an ensemble of initial conditions chosen to reproduce quantum distribution immediately after tunneling. The distributions of velocities and positions along and perpendicular to the laser polarization are obtained by applying the Dykhne method to the tunneling problem, as described in detail in [14]. They are Gaussian in both parallel $v_\parallel$ and perpendicular $v_\perp$ velocity components, with $\Delta v_\parallel = (2E\cos\phi)^{1/3}$ and $\Delta v_\perp = (E\cos\phi/\sqrt{2I_p})^{1/2}$ (see [12] for details). The coordinates have appropriate Fourier-conjugated distributions.

In the model, double ionization is caused by the recollision of the active electron with the parent ion. Its probability is determined by the *total* inelastic cross section σ_{inel} of this collision, which includes not only ionization but also excitation to all states. Excitation followed by prompt laser induced ionization plays a crucial role. Calculations were performed for He because it is the only atom for which there are sufficient theoretical and experimental data for total inelastic cross sections [12].

Calculations were done for the laser wavelength $\lambda = 780$ nm, both for pulses and for constant laser intensity. For pulses longer than 100 fs the results agree with constant intensity calculations. In the latter case one has to start trajectories only during one-half of the laser cycle, with phases of tunneling between $-90°$ and $+90°$. A total of 10^5 trajectories per phase, for 40 different initial phases were propagated. As shown in [12], for $I > 2 \times 10^{14}$ W/cm^2 one can use field-free cross sections of $e + \text{He}^+$ collisions, because the laser field contribution to the phase of the electronic wave function (i.e., the action integral) during the brief time of the hard collision is small [12]. Of course, it is crucial to take the laser field into account before and after the collision. We assume that any real excitation of He^+ states results in eventual 100% ionization by the laser field. This is a valid assumption since all excited states of He^+ are above the Coulomb barrier already at intensities $I > 3.5 \times 10^{13}$ W/cm^2, i.e., more than an order of magnitude less than the intensity range of interest.

To test the model, the calculations were compared to the benchmark experimental data of [11], for $\lambda = 780$ nm and pulse duration 150 fs. Figure 1 shows the $\text{He}^{2+}/\text{He}^+$ ratio as a function of laser intensity. There is quantitative agreement between calculations (upper curve) and the experimental results (circles) [11]. Two phenomena, Coulomb focusing [10] and collisional excitation, have to be included to obtain such good agreement.

The bottom curve in Fig. 1 is obtained using the standard recollision model which ignores both the Coulomb focusing (i.e., sets the core charge to zero) and collisional excitation. As demonstrated by the next curve from the bottom, which includes excitation but still ignores the Coulomb focusing, excitation plays a crucial role in double ionization. Two factors are important. First, the excitation cross sections for $e + \text{He}^+$ collisions are always larger than ionization cross sections (for a typical energy $E \approx$ 100 eV the factor is about 2.8 for the spin-averaged cross section). Second, the onset of excitation occurs at lower energy than ionization. Therefore excitation is even more essential for double ionization at low intensities, when the energy of the recolliding (active) electron is low.

The bottom two curves are virtually insensitive to how many cycles each trajectory is propagated. Indeed, without the Coulomb potential, if the electron misses the parent ion on the first return due to initial $v_\perp$, it will also miss during the subsequent returns. The situation changes dramatically when the Coulomb potential of the parent ion is taken into account. This is illustrated by the upper three curves. The duration of the propagation of each trajectory is indicated at the side of each curve. As trajectories are allowed to propagate for a larger number of laser cycles, the probability of successful inelastic recollision increases. The Coulomb interaction between the electron and the ion reduces the transverse spread of the electronic wave packet, thereby enhancing the probability of the electron revisiting the ion core. The enhancement is clear already during the first laser cycle (compared to the bottom two curves). This modification increases as a result of multiple soft collisions between the electron and ion that occur over the next few laser cycles. Coulomb focusing has little additional impact on double ionization after about ten cycles: by that time virtually all trajectories that will experience hard collision have already done so and left the vicinity of the parent ion for good. For very short pulses, the calculation underestimates the pulse duration sensitivity since we assume that all excited atomic ions will ionize in the strong laser field. In reality, ionization may take a period or more.

Figure 1 clearly implies important few cycle dynamics in intense field double ionization: for sufficiently short pulses, when the electron has only a few laser cycles to find the parent ion, the yield of doubly charged ions should be reduced. Our experiment was aimed at verifying this prediction. Since tunneling of the active electron is most likely at the peak of the pulse, in zero approximation the relevant time scale is the fall time of the pulse.

Experimentally, we demonstrate the pulse duration dependence of double ionization of Ne using 12 and 50 fs, 800 nm pulses (fall times of 2–3 cycles and ~10 cycles). We choose Ne instead of He because Ne has three isotopes ^{20}Ne(90.5%), ^{21}Ne(0.27%), and ^{22}Ne(9.2%) that can be used to achieve a good dynamic range of the signal. The ratio of $^{20}\text{Ne}^+$ to $^{20}\text{Ne}^{2+}$ is about 500 to 1 in the nonsequential ionization region but that of $^{22}\text{Ne}^+$ to $^{20}\text{Ne}^{2+}$ is only 50:1. In addition, the mass resolution of our time-of-flight spectrometer is insufficient to eliminate the possible contribution of H_2^+ to the He^{2+} signal.

The laser system consists of a mode-locked Ti:sapphire oscillator whose output is regeneratively amplified at a repetition rate of 310 Hz to a maximum pulse energy of 500 μJ. To obtain short (12 fs), high-energy pulses [15], the 50 fs pulses from the regenerative amplifier were focused into a 50 cm long hollow core fiber (250 μm inner

diameter) filled with Ar at 1 atm. The spectrum was broadened to ~200 nm FWHM by self-phase modulation. Pulse chirp was removed by two pairs of fused silica prisms (20° apex angle) in double pass geometry to achieve a pulse duration of 12 ± 2 fs and maximum pulse energy of 100 μJ.

Using a 75 cm spherical mirror the M^2 of both 50 and 12 fs beams was measured to be 1.7 ± 0.1 and 1.77 ± 0.14, respectively. This allows us to estimate the focal spot diameter inside the vacuum chamber (base pressure of 10^{-8} Torr) for the 5 cm parabolic mirror which was used to focus the two beams. We estimated the focal spot diameters to be 6 ± 0.3 μm and 5.4 ± 0.4 μm FWHM for 50 and 12 fs pulses, respectively. A fast photodiode measured pulse energy reflected from a 1.5 mm uncoated fused silica beam splitter near normal incidence. The focal spot diameters, measured pulse energies, and estimated durations in the chamber allow one to estimate the peak intensity. However, since ADK (Ammosov, Delone, and Krainov) is accepted to accurately determine the ionization rates for atoms we calibrate the intensities with the ADK intensities. The intensities estimated from the focal diameters had to be lowered by a factor of 2 for both the pulse durations.

The ions were analyzed by a time-of-flight spectrometer described in detail elsewhere [16]. The microchannel plate (MCP) detector was operated in an ion-counting mode in conjunction with a multichannel scaler. We obtained ion yields by integrating the appropriate peaks. Simultaneous collection of Ne^+ and Ne^{2+} signals eliminates possible errors in reproducing pressures in sequential runs. To achieve a high dynamic range without saturating the detection system, we took scans at different pressures and used ^{22}Ne and ^{20}Ne isotopes for singly and doubly charged signals, respectively. As an additional check for some scans we measured the ratio of $^{21}Ne^+$ to $^{20}Ne^{2+}$.

We used a half-wave plate and a polarizer to vary the intensity of 50 and 12 fs pulses. For the 50 fs pulses, both of them were used before the grating compressor. To accommodate the broad bandwidth of a 12 fs pulse we use a half-wave plate before the hollow core fiber to rotate the polarization. It does not change the energy or the pulse duration. Since the system is axially symmetric, self-phase modulation is not affected and the polarization remains linear. We use a germanium slab at Brewster's angle to reflect only the *s* component of the polarization after the fiber.

The nonsequential ionization yield is extremely sensitive to the ellipticity of the laser radiation [7]. Two additional germanium Brewster-angle reflectors just before the target chamber ensure an extinction ratio greater than 300:1.

A broad-bandwidth 12 fs pulse is extremely sensitive to dispersion. To obtain minimum pulse width in the vacuum chamber we must compensate for the dispersion of air, beam splitter (1.5 mm), and vacuum chamber (6 mm) fused silica windows. Since below the saturation intensity, Ne^+ yield is very sensitive to peak intensity and hence pulse duration, at an intensity of 3×10^{14} W/cm^2, we maximize the Ne^+ signal by changing the prism position. After passing through the equivalent amount of air and material of the beam splitter and vacuum chamber windows we also measured the pulse duration to be 12 fs by second harmonic frequency resolved optical gating, using a 10 μm beta-barium borate crystal.

The ion yields are shown as a function of the laser intensity in Fig. 2 for 50 fs pulses. We have reduced the Ne^{2+} signal by a factor of 2.5 ± 0.5 to account for the higher sensitivity of the MCP to Ne^{2+} relative to Ne^+. Also shown are the sequential ionization probabilities calculated using ADK tunneling rates [13] for 50 fs (solid curve) and 12 fs (dashed curve) pulses. Gaussian pulses were assumed in time (FWHM of 50 and 12 fs) and space. Spatial averaging was carried out throughout the focal volume. At a given intensity and therefore a given ionization rate, the yield is reduced for a short pulse. In Figs. 2 and 3 we lower the experimental intensities by a factor of 2 to match the ADK intensities. The large discrepancies in Ne^{2+} yield between the experiment and ADK at lower intensities is a signature of nonsequential double ionization [3].

A convenient way of studying the nonsequential double ionization is by plotting the ratio Ne^{2+}/Ne^+ as a function of laser intensity [11]. The nonsequential ionization region seen in Fig. 2 becomes a plateau when plotted as a ratio (Fig. 3). Sequential ionization causes a deviation from the plateau seen for intensities greater than about 10^{15} W/cm^2.

Figure 3a shows experimental and ADK ratios (solid curves) for the two pulse durations. The experimental ratio of Ne^{2+} to Ne^+ yield for 12 fs pulses (triangles) is

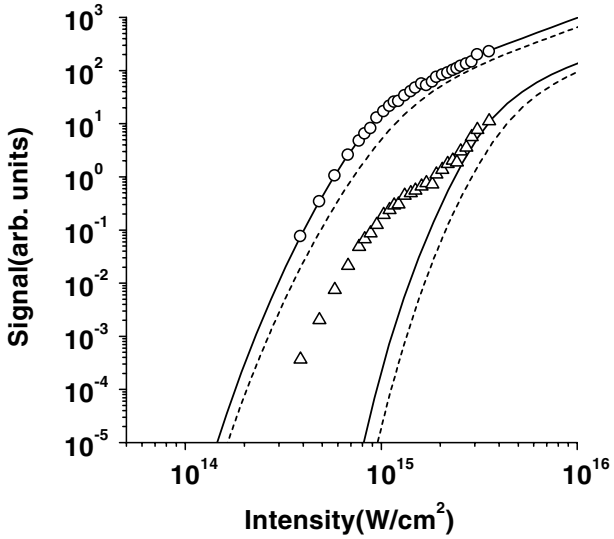

FIG. 2. Yield of singly (circles) and doubly (triangles) charged ions as a function of laser intensity. ADK probabilities for both singly (curve on left) and doubly (curve on right) charged ions were calculated assuming Gaussian pulses with FWHM of 50 fs (solid curves) and 12 fs (dashed curves).

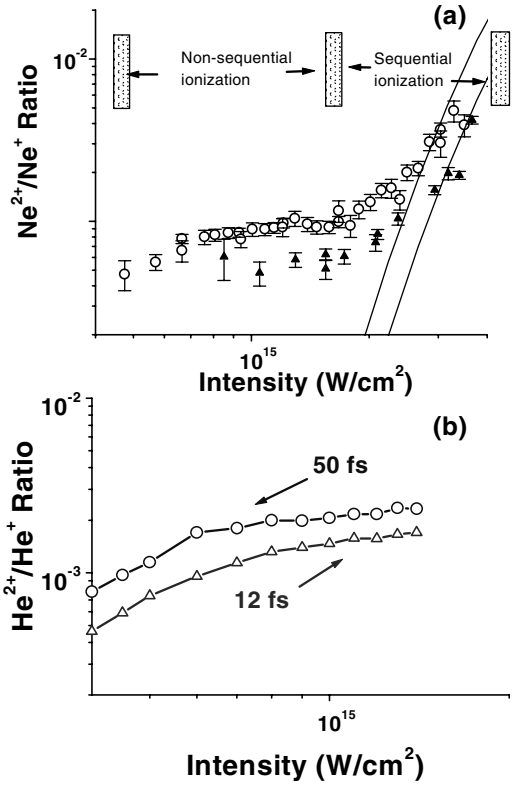

FIG. 3. (a) The ratio of Ne^{2+}/Ne^{+} yields vs peak laser intensity for 50 fs (circles) and 12 fs (triangles) pulses, for $\lambda = 800$ nm. Each data point is an average of 10^5 laser shots. The error bars are statistical. The solid lines are calculated ADK probabilities for 50 fs (left curve) and 12 fs (right curve), respectively. Data are corrected for greater detection efficiency of microchannel plates towards higher charge states. (b) Calculations for He for the same experimental conditions.

$\sim$60% lower than that for 50 fs pulses (circles) indicating a reduction in production of Ne^{2+} with pulses of only a few optical cycles.

From the theoretical perspective, in the recollision model this effect is related to the Coulomb focusing of trajectories on the parent ion after several laser cycles (so-called "late returns"). In short pulses, late returns that occur near the end of the pulse are inefficient due to low collision energy. The relevant time scale is the fall time of the pulse, which is 6 fs in case of 12 fs pulse. Since this effect is general, we expect quantitatively similar results for He and Ne. Results of our calculations for 12 and 50 fs pulses are shown in Fig. 3b. The change in the relative yield predicted by the theory for He ($\sim$0.56–0.73) is close to the experimental value of ($\sim$0.6) for Ne.

In conclusion, we stress several aspects of strong field double ionization. (1) The final yield of nonsequential double ionization is dominated by collisional excitation followed by prompt laser-induced ionization of excited states. This should have observable consequences in the electron spectrum of correlated double ionization [8]. (2) While only hard collisions of the active electron with the parent ion cause excitation and/or ionization, multiple soft collisions during the first few cycles play an important role in determining the final double ionization yield. Consequently, the correlated electron spectrum should change with the laser pulse duration. (3) As a result of these soft collisions, electrons can be transiently trapped in the Rydberg-type orbits. (4) Transiently trapped electrons not only Coulomb focus on the parent ion, but can also acquire a maximum energy of $3.2U_p$ at the moment of hard collision irrespective of the moment of initial tunneling. (5) The wavelength and ellipticity of the laser radiation affect Coulomb focusing. These are control parameters for collisional innershell excitation. Finally, because of the complexity of Coulomb focusing orbits, coherent high harmonic generation is not significantly influenced by anything but the first return.

We acknowledge stimulating discussions with L. DiMauro and are grateful to him for sending us the experimental data of Ref. [11]. M. M. acknowledges financial support from Photonics Research Ontario.

[1] J. S. Briggs and V. Schmidt, J. Phys. B **33**, R1 (2000).
[2] See, for example, J. H. McGuire *et al.,* J. Phys. B **28**, 913 (1995), and references therein.
[3] D. N. Fittinghoff, P. R. Bolton, B. Chang, and K. C. Kulander, Phys. Rev. Lett. **69**, 2642 (1992).
[4] A. Becker and F. H. M. Faisal, J. Phys. B **29**, L197 (1996).
[5] B. A. Zon, Zh. Eksp. Teor. Fiz. **116**, 410 (1999) [J. Exp. Theor. Phys. **89**, 219 (1999)]; U. Eichmann, M. Dorr, M. Maeda, W. Becker, and W. Sandner, Phys. Rev. Lett. **84**, 3550 (2000).
[6] P. B. Corkum, Phys. Rev. Lett. **71**, 1994 (1993).
[7] P. Dietrich, N. H. Burnett, M. Ivanov, and P. B. Corkum, Phys. Rev. A **50**, R3585 (1994).
[8] Th. Weber, H. Geissen, and R. Dorner, Nature (London) **405**, 658 (2000); Th. Weber *et al.,* Phys. Rev. Lett. **84**, 443 (2000).
[9] R. Moshammer *et al.,* Phys. Rev. Lett. **84**, 447 (2000).
[10] T. Brabec , M. Yu. Ivanov, and P. B. Corkum, Phys. Rev. A **54**, R2551 (1996).
[11] B. Walker, B. Sheehy, L. F. DiMauro, P. Agostini, K. J. Schafer, and K. C. Kulander, Phys. Rev. Lett. **73**, 1227 (1994).
[12] G. L. Yudin and M. Yu. Ivanov, Phys. Rev. A **63**, 033404 (2001).
[13] M. V. Ammosov, N. B. Delone, and V. P. Krainov, Zh. Eksp. Teor. Fiz. **91**, 2008 (1986) [Sov. Phys. JETP **64**, 1191 (1986)]; N. B. Delone and V. P. Krainov, *Multiphoton Processes in Atoms* (Springer, Berlin, 1994).
[14] N. B. Delone and V. P. Krainov, J. Opt. Soc. Am. B **8**, 1207 (1991).
[15] M. Nisoli, S. De Silvestri, and O. Svelto, Appl. Phys. Lett. **68**, 2793 (1996).
[16] P. Dietrich, D. T. Strickland, M. Laberge, and P. B. Corkum, Phys. Rev. A **47**, 2305 (1993).